Available online at www.sciencedirect.com
SCIENCE DIRECT®
Biochemical and Biophysical Research Communications 332 (2005) 640–645
BBRC
www.elsevier.com/locate/ybbrc

2.0 Å crystal structure of human ARL5-GDP3′P, a novel member of the small GTP-binding proteins

Zhan-Xin Wang, Liang Shi, Jun-Feng Liu, Xiao-Min An, Wen-Rui Chang, Dong-Cai Liang *

National Key Laboratory of Biomacromolecules, Institute of Biophysics, Chinese Academy of Sciences, 15 Datun Road, Chaoyang District, Beijing 100101, PR China

Received 27 April 2005
Available online 10 May 2005

Abstract

ARL5 is a member of ARLs, which is widespread in high eukaryotes and homologous between species. But no structure or biological function of this member is reported. We expressed, purified, and resolved the structure of human ARL5 with bound GDP3′P at 2.0 Å resolution. A comparison with the known structures of ARFs shows that besides the typical features of ARFs, human ARL5 has specific features of its own. Bacterially expressed human ARL5 contains bound GDP3′P which is seldom seen in other structures. The hydrophobic tail of the introduced detergent Triton X-305 binds at the possible myristoylation site of Gly^2, simulating the myristoylated state of N-terminal amphipathic helix in vivo. The structural features of the nucleotide binding motifs and the switch regions prove that ARL5 will undergo the typical GDP/GTP structural cycle as other members of ARLs, which is the basis of their biological functions.

Keywords: ADP ribosylation factor-like protein; GTP-binding; Crystal structure; Guanosine 5′-diphosphate-3′-monophosphate; Myristoylation

ARFs are a family of Ras-related GTP-binding proteins [1]. ARLs [2] belong to the subfamily of ARFs and share 40–60% primary sequence identity to that of ARFs. At least six ARFs and eight ARLs comprise this small G-protein family. Existing studies on ARFs indicate that they show diverse functions in many organelles. ARF1 regulates the recruitment of vesicle coat polymers to the Golgi apparatus [3]; ARF6 coordinates endocytotic membrane traffic with aspects of cytoskeleton organization [3,4]; ARL1 regulates Golgi structure and functions [5–7]. These functions depend on the release of the tightly bound GDP which is catalyzed by appropriate guanine exchange factors (GEFs) and the hydrolysis of GTP which is stimulated by the GTPase-activating proteins (GAPs) [8]. Solved structures reveal that ARFs fold into a conservative structure [9–17]. Most of these members undergo the typical GDP/GTP structural cycle, which is adapted to their functions. ARL5 is widespread in high eukaryotes [18,19]. They are homologous between species, but we do not have any related structural or biochemical information. The structure of human ARL5 can help us reveal the structural features of this subfamily and the possible conformational change during the GDP/GTP structural cycle, which is the basis of their biological functions in vivo.

Materials and methods

Cloning, expression, and purification. Cloning of the gene encoding human ARL5 was carried out by the Shanghai Institute of Hematology. The amplified gene was cloned into pET22b (+) (Novagen)

* Corresponding author. Fax: +86 10 64889867.
E-mail address: dcliang@sun5.ibp.ac.cn (D.-C. Liang).

0006-291X/$ - see front matter © 2005 Elsevier Inc. All rights reserved.
doi:10.1016/j.bbrc.2005.04.168

between the restriction sites of *Nco*I and *Xho*I. The expression vector pET-ARL5 added a C-terminal His_6 tag and linker peptide to the expression protein. The construction was confirmed by DNA sequencing. ARL5 was expressed in *E. coli* stain B834(DE3) (Novagen) after induction with 0.5 mM isopropyl-β-D-thiogalactopyranoside (IPTG) for 4 h at 37 °C. The cells were harvested by centrifugation and were lysed with a cell disrupter. Soluble fraction was loaded on a 5 ml Chelating Sepharose Fast Flow resin loaded with $NiSO_4$ and pre-equilibrated in 50 mM Tris–HCl (pH 8.0), 500 mM NaCl, and 20 mM imidazole. After three washes with increasing concentrations of imidazole (20, 50, and 100 mM), the bound protein was eluted with 300 mM imidazole. Proteins eluted from the resin were further purified to high homology by size exclusion chromatography on Superdex 200 column (Amersham Biosciences).

Crystallization and data collection. Human ARL5 was crystallized using the hanging-drop, vapor diffusion method. Screening experiments were performed with commercial kit Screens 1 and 2 from Hampton Research. Microcrystals were obtained in 0.1 M sodium acetate (pH 4.6), 1.5 M ammonium sulfate. The crystals were first urchin like clusters, without definite shape. By tuning pH finely and adding detergents, we finally got the single rod like crystals from a protein solution of 10 mg/ml mixed in a 1:1 ratio with well solution containing 0.1 M sodium citrate (pH 5.3), 1.4 M ammonium sulfate, and 0.1% Triton X-305 at 15 °C. We did not introduce any GDP molecules or magnesium ions during the crystallization process. The crystals grew to about $0.4 \times 0.06 \times 0.06\ mm^3$ within a week.

Diffraction data were collected at Spring-8 (Himeji, Japan) and Photon Factory (Tsukuba, Japan). They were integrated and scaled with DENZO and SCALEPACK from the HKL program suite [20]. The results show that the crystal belongs to the space group I222/I212121 (finally identified as I212121), with one molecule in the crystallographic asymmetric unit. The diffraction data statistics are summarized in Table 1.

Structure determination and refinement. The structure was solved by molecular replacement with MolRep [21] in the CCP4 [22] suite. The search model was the structure of rat ARF1 (PDB entry 1RRG), which displays 49% sequence identity with human ARL5. The initial model was manually rebuilt with the program O [23] and refined with CNS [24]. The refined model was put into ARP/wARP [25], resulting in a partially docked model. The new model was further refined with CNS and rebuilt with O. After several cycles of refinement, we obtained the final model. A summary of the refinement statistics is given in Table 1. The coordinates and structure factors for human ARL5-GDP3′P have been deposited in the RCSB Protein Data Bank with accession code 1ZJ6.

Structure analysis and figure preparation. The structure alignments and r.m.s.d calculations were performed by O. The molecule surface was drawn by GRASP [26]. Structure and electron density representations were drawn by MolScript [27], rendered by Raster3D [28].

Table 1
Crystal data, data collection, and refinement statistics

Space group	I212121
Unit cell parameters (Å)	
a	76.8
b	81.5
c	84.6
Molecules (a.u.)	1
Mosaicity (°)	0.45
Resolution range (Å)	50.00–2.00 [2.06–2.00][a]
Unique reflections	16149
Average redundancy	5.5
Completeness	88% [91%]
R_{merge} (%)	0.091 [0.44]
$I/\sigma(I)$	34.1 [3.3]
Non-hydrogen atoms	1403
Amino-acid residues	173
Sulfate ions	2
Water molecules	114
R_{work} (%)	21.2%
R_{free} (%)	22.2%
r.m.s.d. bond lengths (Å)/angles (°)	0.007/1.44
Average *B*-values (Å^2) for main chain/sidechain/water/sulfate ions/GDP3′P	29.6/34.2/36.3/27.3/28.3

[a] Numbers in parentheses correspond to the highest-resolution shell.

Results and discussion

Overall structure

The structure of human ARL5-GDP3′P complex has been determined to a resolution of 2.0 Å by X-ray diffraction using molecular replacement. The core of this structure is a six-stranded β-sheet surrounded by five α helices, linked by loops and three 3_{10} helices. It exhibits the typical fold of ARFs and has the typical components of this family: the N-terminal amphipathic α helix that rests at the hydrophobic pocket between the C-terminal helix and the interswitch [13,19] region; two switch regions (switch I and switch II) that interact with the effectors when they are in their active GTP-bound form; the interswitch region which transmits the conformational change during the GDP/GTP structural cycle. Human ARL5 gene encodes 179 amino acids, the crystal structure showing it as a monomer. The refined model includes residues from 2 to 178 (missing residues from 70 to 73 which are located at the loop region and where the electron density is poor) one molecule of guanosine 5′-diphosphate-3′-monophosphate (GDP3′P), two sulfate ions, and 114 ordered water molecules. The overall structure is shown in Fig. 1.

Bacterially expressed human ARL5 contains bound GDP3′P

The higher affinity for GDP over GTP and lipid dependence on the binding of activation guanine nucleotides likely explain the presence of GDP in the nucleotide binding site of ARFs as purified from mammalian tissues or bacteria [29]. We did not introduce any GDP molecules in the crystallization trials, but the solved structure shows distinct positive density at the GDP-binding site. During model rebuilding and refinement, a well-defined mass of $2F_o - F_c$ and $F_o - F_c$ density within the sequence from Gly^{23} to Lys^{29} (P-loop) clearly indicated the presence of a small molecule. We put one GDP molecule into the nucleotide binding site; it fitted well into the density, except that there was still a clear, unfilled positive density at the 3′ position of the ribose. Composite omit map confirmed the continuous density as well. The distance from the center of the density to the 3′ hydroxyl suggests that the 3′ ribose is covalently modified by an additional phosphate as referred

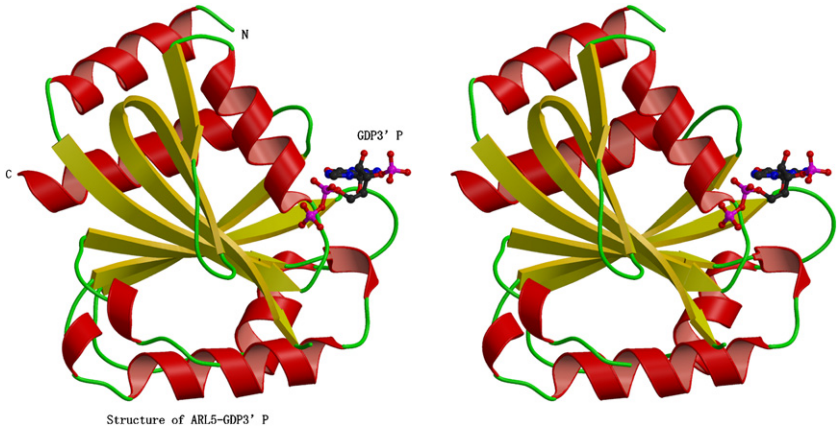

Fig. 1. A stereo view of the human ARL5-GDP3′P. We colored the α helices red, β-strands yellow, and the coils green. GDP3′P is shown in ball-and-stick representation. (For interpretation of the references to colour in this figure legend, the reader is referred to the web version of this paper.)

[12]. $2F_o - F_c$ and $F_o - F_c$ maps rebuilt with GDP3′P as ligand exhibited no positive or negative density at the nucleotide binding site. See Fig. 2 for details. This is another evidence that GDP3′P is a natural ligand of ARLs. GDP3′P involves in the stringent responses in *E. coli* [30,31]. We do not know of its biological significance in eukaryotes; but from the structure we can see that the modified phosphate points to the solvent region and is not involved in any electrostatic interactions. So we can predict that as the analog of GDP, GDP3′P can bind other ARLs with high affinity. It can compete for the binding site at the nucleotide binding pocket with GDP, and it may be a universal substrate of these proteins. That GDP3′P plays a similar or opposite role when taking the place of GDP remains to be proved. But it provides us with a clue in devising small medical substrate to these proteins. By covalently modifying the 3′ position of the ribose, we can produce the competitive substrate to ARLs, which suggests a possible way to regulate these proteins.

N-terminal switch and the myristoyl motif

ARF1 interacts with the membrane through its amphipathic N-terminal helix [32], which is also called the N-terminal switch. The N-terminal switch is very important, because it regulates the structural cycle and the spatial cycle of the protein. Corresponding to the GDP/GTP structural cycle, ARFs undergo the spatial cycle of moving between the cytoplasm in GDP-bound form and anchored to the membrane in GTP-bound form. The N-terminal switch interacts with the membrane through two components: one is the myristoyl motif at Gly^2 by myristoylation. Myristoylation irreversibly adds a saturated C:14 fatty acid to the N-terminal glycines of some ARFs. The long hydrophobic tail of the myristate gives a basal affinity for the lipid regardless of the protein conformation. The other is the clusters of hydrophobic residues of the N-terminal helix, whose sidechains insert into the membrane when dissociated from the pocket in active GTP-bound state. But

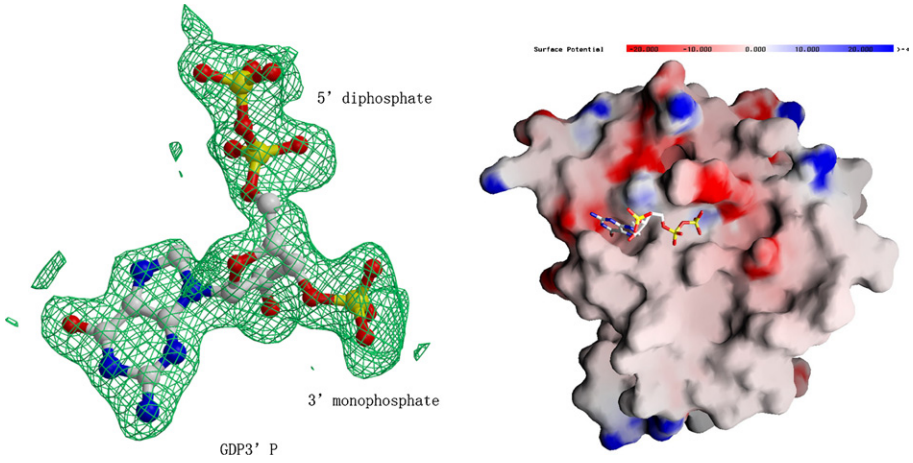

Fig. 2. Left is an electron-density map of GDP3′P. The $2F_o - F_c$ map is shown contoured at 1σ level. Right is a GRASP model showing the electrostatic surface of ARL5. GDP3′P is drawn in ball-and-stick model. We colored carbon atoms white, oxygen atoms red, nitrogen atoms blue, and the phosphate atoms yellow. (For interpretation of the references to colour in this figure legend, the reader is referred to the web version of this paper.)

we still need to determine the structural features that account for stable existence of saturated C:14 hydrophobic tail in the cytoplasm in GDP-bound form and its rapid switch to the affinitive form when approaching the membrane. The N-terminal myristoylation site of human ARL5 is circled by the tail of the crystallization detergent Triton X-305, mimicing the natural confirmation of myristate, providing us a visual explanation to the question mentioned above. Myristoylation occurs at the N-terminal glycine [33], which means that the encoded N-terminal methionine was excised during the expression. We propose that human ARL5 is myristoylated in native form. The high similarities of N-terminal sequence with that of ARF1 (which is myristoylated at the N-terminal glycine) and the hydrophobic environment around the N-terminus make it possible. Expressed human ARL5 starts from Gly^2, which is necessary for myristoylation. Furthermore, the N-terminal glycine is circled by a well-defined, half-ring-shaped density. The density is evident even when the $F_o - F_c$ map is contoured at the 3σ level. It has the shape of a detergent tail, but not the shape of any residue. We happened to add Triton X-305 in the crystallization process, which is a key component in crystal optimization. As the tail of Triton X-305 is similar to that of Triton X-100, except the difference in length, we used the known structure of Triton X-100 as model, filled just 14 atoms (–C–C–O–C–C–O–C–C–O–C–C–O–C–C–) into the density, corresponding to the 14 carbon atoms of myristate. The final result is illustrated in Fig. 3. The conformation of the detergent tail reveals how it can be stable while keeping a basal affinity to the membrane. The hydrophobic tail is like a rope firmly wrapping the terminal glycine, but not extending freely into the solvent region as we had expected. The half-ring-shaped confirmation lowers the free energy by burying most of the hydrophobic atoms in the hydrophobic pocket. This conformation also facilitates the end of myristate to disassociate from the gap of the half ring and keep a basal affinity to the membrane. It is the first structure that illustrates a possible conformation of myristoylation at N-terminal glycine in ARLs.

As the least hydrophobic lipid modification [32,34], myristoylation alone cannot explain the GTP dependent hydrophobic interaction between ARFs and the membrane. It is rather weak and dissociates quickly, but is strengthened when the sidechains of N-terminal hydrophobic residues are inserted into the membrane. Comparing the N-terminal sequence of ARL5 with that of ARF1, we find that it exhibits more hydrophobicity with the three clusters of hydrophobic components L^4F^5, I^8W^9, and $L^{11}F^{12}$. N-terminal sequence alignment is shown in Fig. 3. Replacement of Phe^9 of ARF1 with Trp^9 (which is the counterpart in ARL5) increases the affinity of N-terminus for the lipids [32]. In addition to the insertion of hydrophobic sidechains, the long sidechains of the following polar residues are responsible for the non-specific electrostatic interactions. The above evidences reveal that the N-terminus of human ARL5 plays an important role in the GDP/GTP structural cycle.

Key motifs in the GDP/GTP cycle

It is well illustrated that ARFs exhibit functional cycle during the GDP/GTP structural cycle. The process involves the exchange of GDP for GTP and is in principle reversible. The bound GTP can be hydrolyzed to GDP with the help of GAPs, which is irreversible. Does ARL5 undergoes this GDP/GTP structural cycle? What

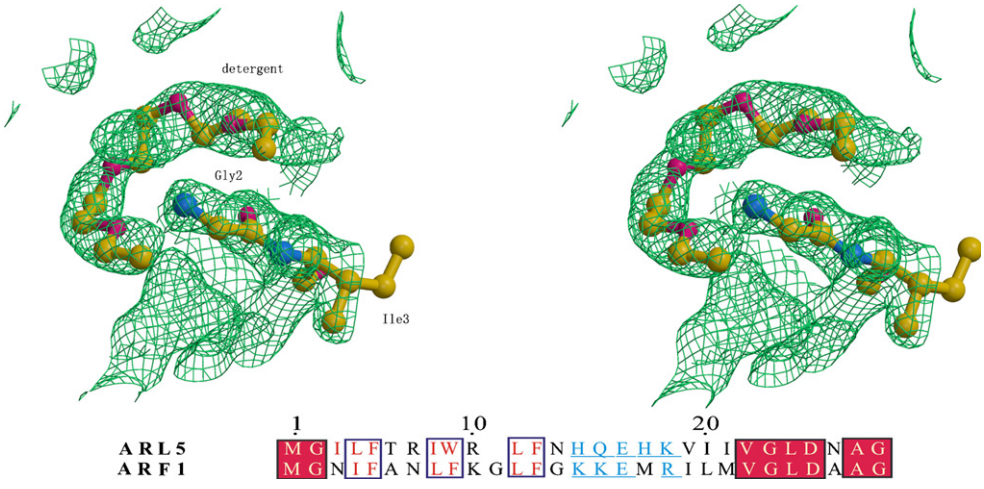

Fig. 3. Above is a stereo view of the additional electron density around the N-terminal glycine. We filled 14 atoms (10 carbon atoms and four oxygen atoms) of the hydrophobic tail of Triton X-305 into the density. We colored the carbon atoms yellow, the oxygen atoms red, and the nitrogen atoms blue. Below is the N-terminal sequence alignment of human-ARL5 and rat-ARF1. (For interpretation of the references to colour in this figure legend, the reader is referred to the web version of this paper.)

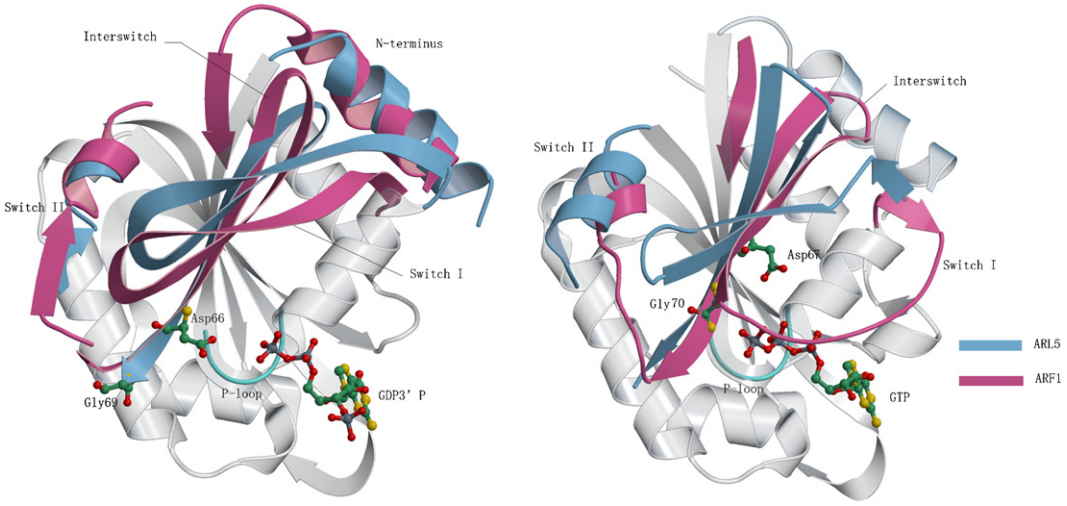

Fig. 4. Left: the overlapped structures of ARL5-GDP3′P and ARF1-GDP. We only kept the N-terminus, switch regions, and interswitch region of ARF1, and colored them purple. We colored the corresponding parts of ARL5 light blue and the remaining parts white. GDP3′P, Gly^{69}, and Asp^{66} of ARL5 are represented in ball-and-stick model. Right: the overlapped structures of ARL5-GDP3′P and ARF1-GTP. The structures were represented the same way as the left. GTP, Gly^{70}, and Asp^{67} of ARF1 are represented in ball-and-stick model. (For interpretation of the references to colour in this figure legend, the reader is referred to the web version of this paper.)

are the structural elements that make this cycle possible? Comparing the ARL5 structure with the known structures of ARF1-GDP, ARF6-GDP, and their GTP bound forms, we found that two key motifs contribute to the structural cycle. One is the GLDxxGK motif (in ARL5 is GLDNAGK), called P-loop [35]. During the cycle, GDP/GTP rests at the highly conserved polar pocket which changes less and holds the nucleotide tightly via hydrogen bonds. The other key motif is the DxGGQ motif (in ARL5 is DIGGQ) upstream of switch II. We may call it a movable lid. It covers the top of the pocket constructed by P-loop, facing the 5′ phosphate of the nucleotide. During the GDP/GTP cycle, the lid moves accordingly to adjust the space between the 5′ phosphate and the lid, so that the pocket can hold the nucleotide firmly. In ARL5, the conserved Asp^{66} in the motif occupies the position just opposite the β-phosphate of GDP, leaving no room for binding the γ-phosphate of GTP. When activated, the interswitch will undergo a two-residue register shift that pulls the two tandem glycines to the place of Asp^{66}, making enough room to facilitate GTP binding. The structure of the key motif P-loop is very conservative throughout this family [36]. These two key motifs altogether compose the structural basis of the GDP/GTP cycle.

Variations in the switch regions

ARFs interact with GEFs through their switch regions mainly in a hydrophobic manner [9,16,17]. Comparing with the structure of ARF1-GTP, we may define switch I of ARL5 as the region comprising residues Met^{38} to Ser^{50}, and switch II is formed by residues Asp^{66} to Thr^{82}. Compared with the structure of ARF1-GDP, the switch regions of ARL5 show the highest variation (r.m.s.d = 2.1 Å in switch I region and 1.9 Å in switch II region), while residues from Asn^{83} to Arg^{175} converge to very similar structures (r.m.s.d = 0.72 Å). These structural differences explain their specificity in target protein selection. Comparing ARL5-GDP with GTP-bound ARFs, we can uncover that the switch I region undergoes the most remarkable conformational change. In human ARL5, part of switch I is folded into a β-strand that forms part of the central β-sheet core. This ordered structure is further stabilized by the N-terminal amphipathic helix. In ARF1-GTP, with the release of the N-terminus, the auxiliary hydrophobic interaction disappears, switch I exhibits a relax conformation, exposing a larger contact surface. What's more, this extended conformation eliminates steric hindrance in GEF binding. Switch II changes less during its interaction with GEFs, but confers the main recognition surface. We did not construct the residues of ARL5 from Gln^{70} to Leu^{73} where the electron density is poor. The region does not form an ordered structure, which is consistent with its property as the specific recognition site. Structural alignment of ARL5 and ARF1 is shown in Fig. 4.

Acknowledgments

This work was supported by the National Natural Science Foundation of China (NSFC) Nos. 30130080, 30200046; 973 Project No. 2004CB520801; 863 Program No. 2002BA711A13, KSCX1-SW-17, and KJCX2-SW-N06 from the Ministry of Science and Technology of China (MOST) as well as funds from CAS. We thank

Dr. Chun-Jung Chen, Prof. N. Sakabe, and Dr. K. Sakabe for their help during diffraction data collection.

References

[1] R.A. Kahn, A.G. Gilman, Purification of a protein cofactor required for ADP-ribosylation of the stimulatory regulatory component of adenylate cyclase by cholera toxin, J. Biol. Chem. 259 (1984) 6228–6234.
[2] J.W. Tamkun, R.A. Kahn, M. Kissinger, B.J. Brizuela, C. Rulka, M.P. Scott, J.A. Kennison, The arflike gene encodes an essential GTP-binding protein in *Drosophila*, Proc. Natl. Acad. Sci. USA 88 (1991) 3120–3124.
[3] P. Chavrier, B. Goud, The role of ARF and Rab GTPases in membrane transport, Curr. Opin. Cell Biol. 11 (1999) 466–475.
[4] C. Souza-Schorey, G. Li, M.I. Colombo, P.D. Stahl, A regulatory role for ARF6 in receptor-mediated endocytosis, Science 267 (1995) 1175–1178.
[5] L. Lu, H. Horstmann, C. Ng, W. Hong, Regulation of Golgi structure and function by ARF-like protein 1 (Arl1), J. Cell Sci. 114 (2001) 4543–4555.
[6] S.L. Lowe, S.H. Wong, W. Hong, The mammalian ARF-like protein 1 (Arl1) is associated with the Golgi complex, J. Cell Sci. 109 (Pt. 1) (1996) 209–220.
[7] V.H. Van, J.F. Shern, J.D. Sharer, X. Zhu, R.A. Kahn, ADP-ribosylation factors (ARFs) and ARF-like 1 (ARL1) have both specific and shared effectors: characterizing ARL1-binding proteins, J. Biol. Chem. 276 (2001) 22826–22837.
[8] J.G. Donaldson, C.L. Jackson, Regulators and effectors of the ARF GTPases, Curr. Opin. Cell Biol. 12 (2000) 475–482.
[9] M. Hanzal-Bayer, L. Renault, P. Roversi, A. Wittinghofer, R.C. Hillig, The complex of Arl2-GTP and PDE delta: from structure to function, EMBO J. 21 (2002) 2095–2106.
[10] R.C. Hillig, M. Hanzal-Bayer, M. Linari, J. Becker, A. Wittinghofer, L. Renault, Structural and biochemical properties show ARL3-GDP as a distinct GTP binding protein, Struct. Fold. Des. 8 (2000) 1239–1245.
[11] S. Pasqualato, J. Menetrey, M. Franco, J. Cherfils, The structural GDP/GTP cycle of human Arf6, EMBO Rep. 2 (2001) 234–238.
[12] J.C. Amor, J.R. Horton, X. Zhu, Y. Wang, C. Sullards, D. Ringe, X. Cheng, R.A. Kahn, Structures of yeast ARF2 and ARL1: distinct roles for the N terminus in the structure and function of ARF family GTPases, J. Biol. Chem. 276 (2001) 42477–42484.
[13] J.C. Amor, D.H. Harrison, R.A. Kahn, D. Ringe, Structure of the human ADP-ribosylation factor 1 complexed with GDP, Nature 372 (1994) 704–708.
[14] J. Menetrey, E. Macia, S. Pasqualato, M. Franco, J. Cherfils, Structure of Arf6-GDP suggests a basis for guanine nucleotide exchange factors specificity, Nat. Struct. Biol. 7 (2000) 466–469.
[15] S.E. Greasley, H. Jhoti, C. Teahan, R. Solari, A. Fensome, G.M. Thomas, S. Cockcroft, B. Bax, The structure of rat ADP-ribosylation factor-1 (ARF-1) complexed to GDP determined from two different crystal forms, Nat. Struct. Biol. 2 (1995) 797–806.
[16] J. Goldberg, Structural basis for activation of ARF GTPase: mechanisms of guanine nucleotide exchange and GTP-myristoyl switching, Cell 95 (1998) 237–248.
[17] M. Wu, L. Lu, W. Hong, H. Song, Structural basis for recruitment of GRIP domain golgin-245 by small GTPase Arl1, Nat. Struct. Mol. Biol. 11 (2004) 86–94.
[18] M. Breiner, A. Schurmann, W. Becker, H.G. Joost, Cloning of a novel member (ARL5) of the ARF-family of Ras-related GTPases, Biochim. Biophys. Acta 1308 (1996) 1–6.
[19] S. Pasqualato, L. Renault, J. Cherfils, Arf, Arl, Arp and Sar proteins: a family of GTP-binding proteins with a structural device for 'front-back' communication, EMBO Rep. 3 (2002) 1035–1041.
[20] Z. Otwinowski, Oscilation data reduction program, in: L. Sawyer, N. Isaacs, S. Bailey (Eds.), CCP4 Study Weekend: Data Collection and Processing, Daresbury Laboratory, Warrington, UK, 1993, pp. 56–62.
[21] A. Vagin, A. Teplyakov, MOLREP: an automated program for molecular replacement, J. Appl. Cryst. 30 (1997) 1022–1025.
[22] Collaborative Computational Project Number 4, The CCP4 suite: programs for protein crystallography, Acta Crystallogr. D 50 (1994) 760–763.
[23] T.A. Jones, J.Y. Zou, S.W. Cowan, M. Kjeldgaard, Improved methods for building protein models in electron density maps and the location of errors in these models, Acta Crystallogr. A 47 (Pt. 2) (1991) 110–119.
[24] A.T. Brunger, P.D. Adams, G.M. Clore, W.L. DeLano, P. Gros, R.W. Grosse-Kunstleve, J.S. Jiang, J. Kuszewski, M. Nilges, N.S. Pannu, R.J. Read, L.M. Rice, T. Simonson, G.L. Warren, Crystallography and NMR system: a new software suite for macromolecular structure determination, Acta Crystallogr. D. Biol. Crystallogr. 54 (Pt. 5) (1998) 905–921.
[25] A. Perrakis, R. Morris, V.S. Lamzin, Automated protein model building combined with iterative structure refinement, Nat. Struct. Biol. 6 (1999) 458–463.
[26] A. Nicholls, K. Sharp, B. Honig, Proteins Struct. Funct. Genet. 11 (1991) 281–296.
[27] P.J. Kraulis, MOLSCRIPT: a program to produce both detailed and schematic plots of protein structures, J. Appl. Crystallogr. 24 (1991) 946–950.
[28] E.A. Merritt, M.E. Murphy, Raster3D Version 2.0. A program for photorealistic molecular graphics, Acta Crystallogr. D. Biol. Crystallogr. 50 (1994) 869–873.
[29] R.A. Kahn, C. Goddard, M. Newkirk, Chemical and immunological characterization of the 21-kDa ADP-ribosylation factor of adenylate cyclase, J. Biol. Chem. 263 (1988) 8282–8287.
[30] C.C. Pao, P.P. Dennis, J.A. Gallant, Regulation of ribosomal and transfer RNA synthesis by guanosine 5′-diphosphate-3′-monophosphate, J. Biol. Chem. 255 (1980) 1830–1833.
[31] C.C. Pao, J. Gallant, A new nucleotide involved in the stringent response in *Escherichia coli*. Guanosine 5′-diphosphate-3′-monophosphate, J. Biol. Chem. 254 (1979) 688–692.
[32] B. Antonny, S. Beraud-Dufour, P. Chardin, M. Chabre, N-terminal hydrophobic residues of the G-protein ADP-ribosylation factor-1 insert into membrane phospholipids upon GDP to GTP exchange, Biochemistry 36 (1997) 4675–4684.
[33] B. Boisson, C. Giglione, T. Meinnel, Unexpected protein families including cell defense components feature in the *N*-myristoylome of a higher eukaryote, J. Biol. Chem. 278 (2003) 43418–43429.
[34] S. Shahinian, J.R. Silvius, Doubly-lipid-modified protein sequence motifs exhibit long-lived anchorage to lipid bilayer membranes, Biochemistry 34 (1995) 3813–3822.
[35] A. Valencia, P. Chardin, A. Wittinghofer, C. Sander, The ras protein family: evolutionary tree and role of conserved amino acids, Biochemistry 30 (1991) 4637–4648.
[36] J. Cherfils, P. Chardin, GEFs: structural basis for their activation of small GTP-binding proteins, Trends Biochem. Sci. 24 (1999) 306–311.